

A Hypoxia-targeting and Hypoxia-responsive Nano-probe for Tumor Detection and Early Diagnosis

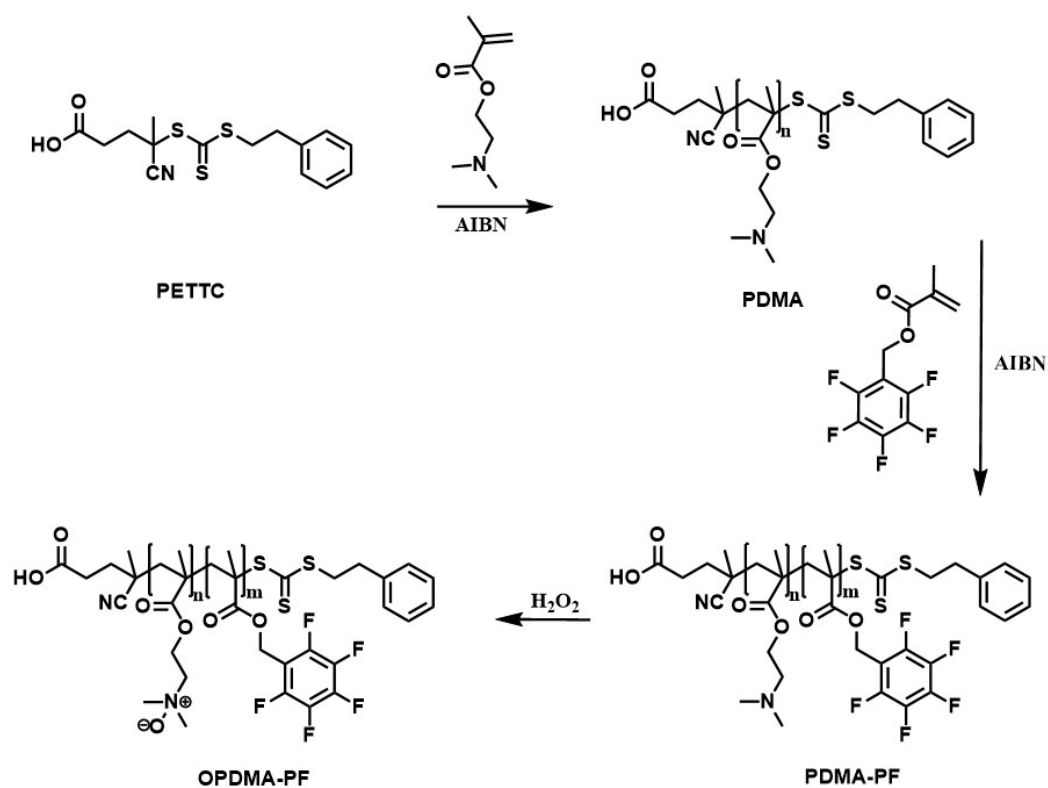
Yong Chen^{a,b#}, Huimin Wang^{b#}, Xiaodan Xu^{c#}, Hongxia Xu^a, Bing Xiao^a, Pengcheng Yuan^b, Shiqun Shao^{a,b}, Wenjing Sun^b, Zhuxian Zhou^a, Youqing Shen^a, and Jianbin Tang^{a,b*}

^a Zhejiang Key Laboratory of Smart BioMaterials, and College of Chemical and Biological Engineering, Zhejiang University, Hangzhou 310058, China

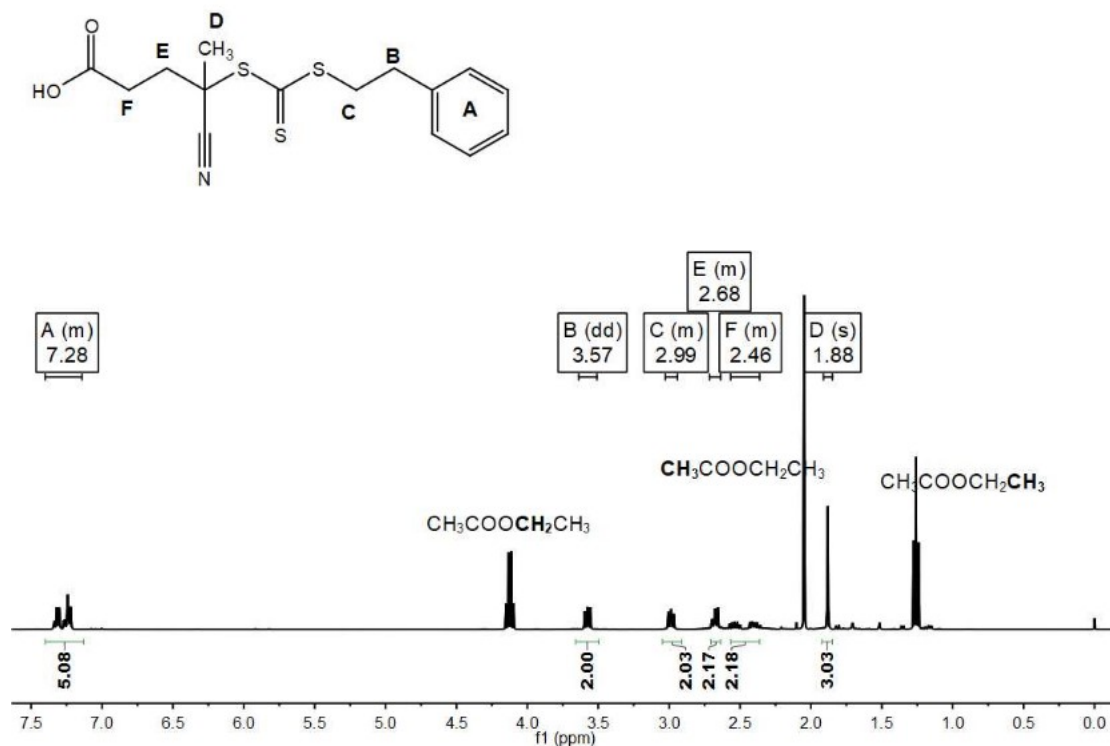
^b ZJU-Hangzhou Global Scientific and Technological Innovation Center, Hangzhou 311215, China

^c Department of Ultrasound in Medicine, Research Center of Ultrasound in Medicine and Biomedical Engineering, The Second Affiliated Hospital of Zhejiang University School of Medicine, Zhejiang University, Hangzhou 310009, China.

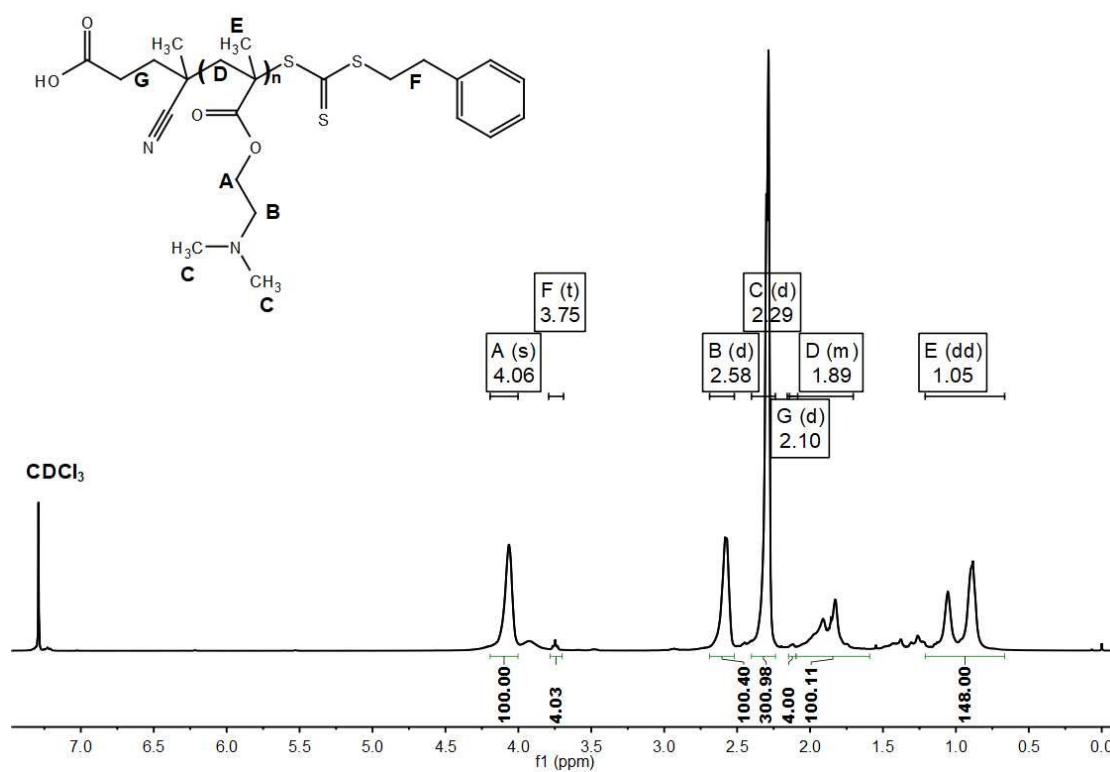
Email: jianbin@zju.edu.cn



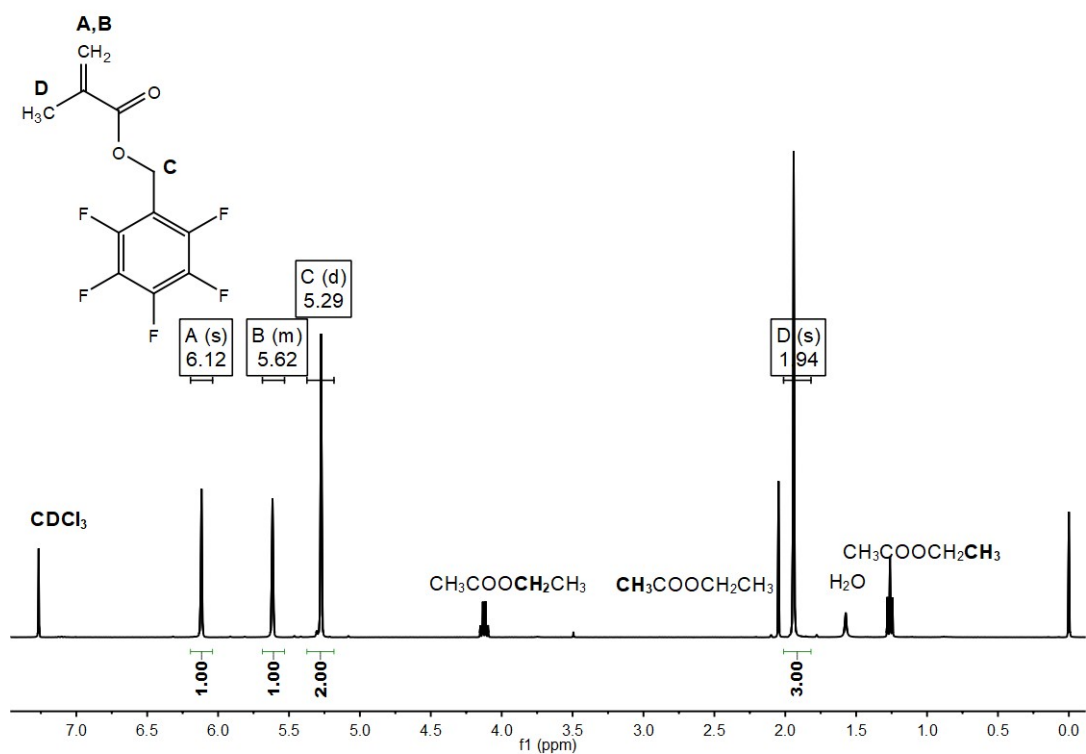
Supplementary Figure S1. Synthesis procedure of OPDMA-PF.



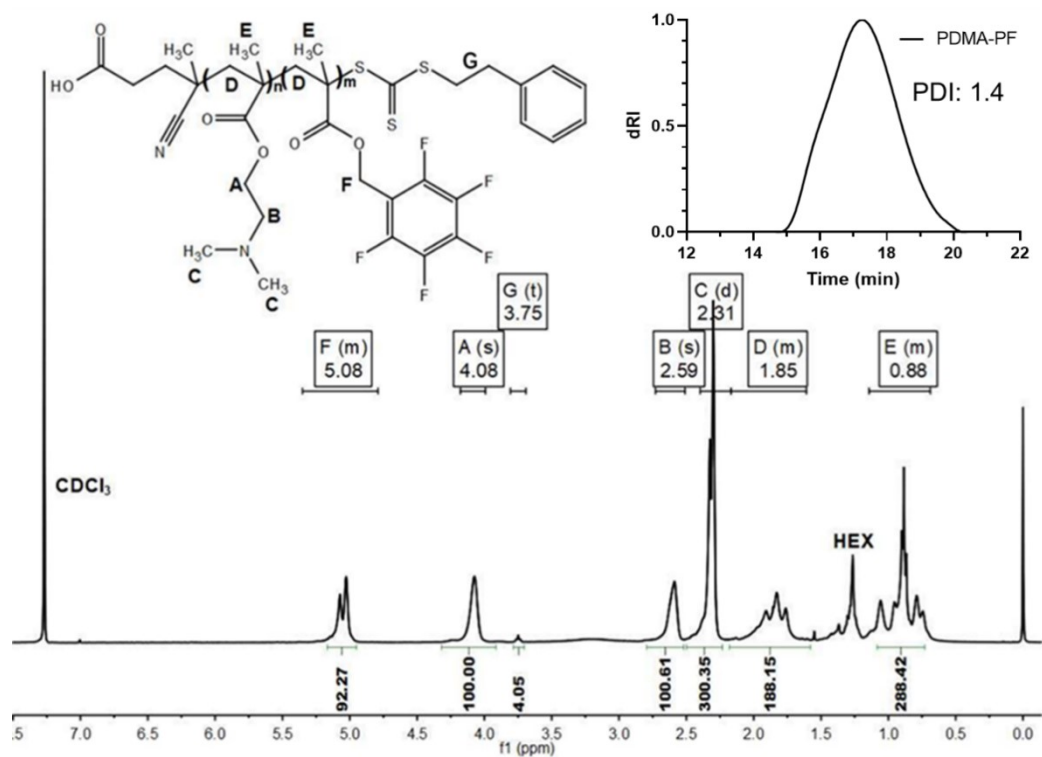
Supplementary Figure S2. ¹H NMR spectra of PETTC (400 MHz, CDCl₃).



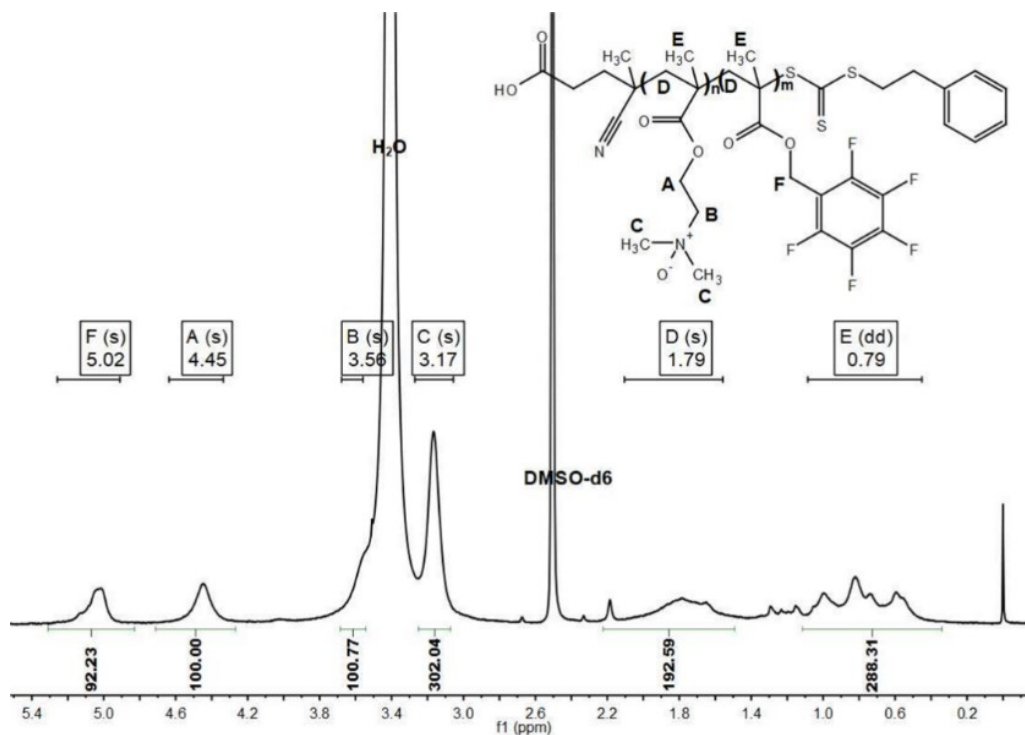
Supplementary Figure S3. ¹H NMR spectra of PDMA (400 MHz, CDCl₃).



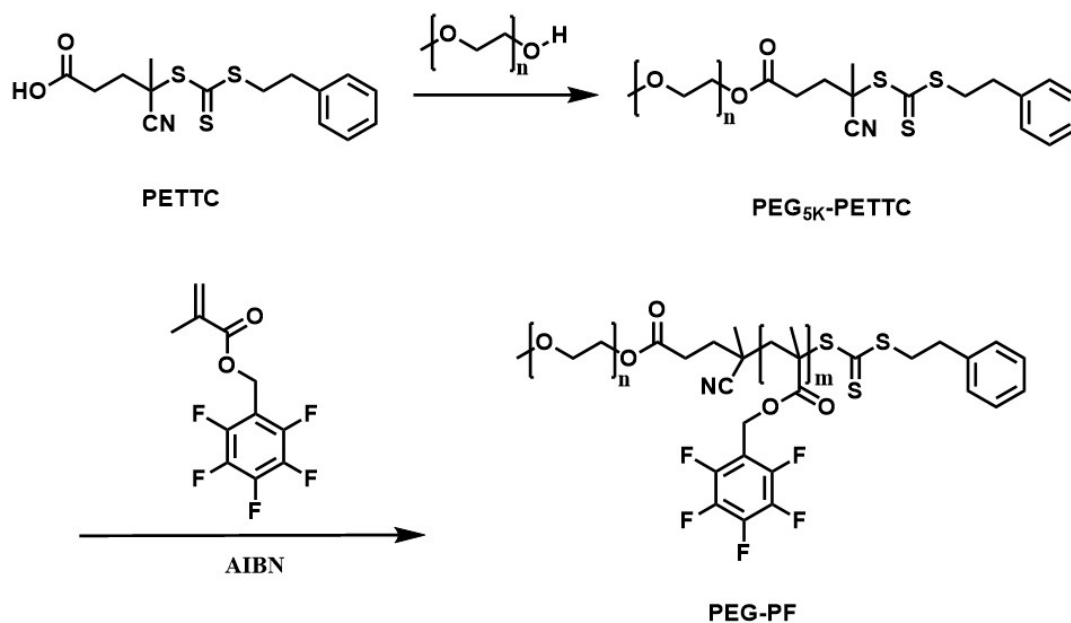
Supplementary Figure S4. ^1H NMR spectra of FBMA (400 MHz, CDCl_3).



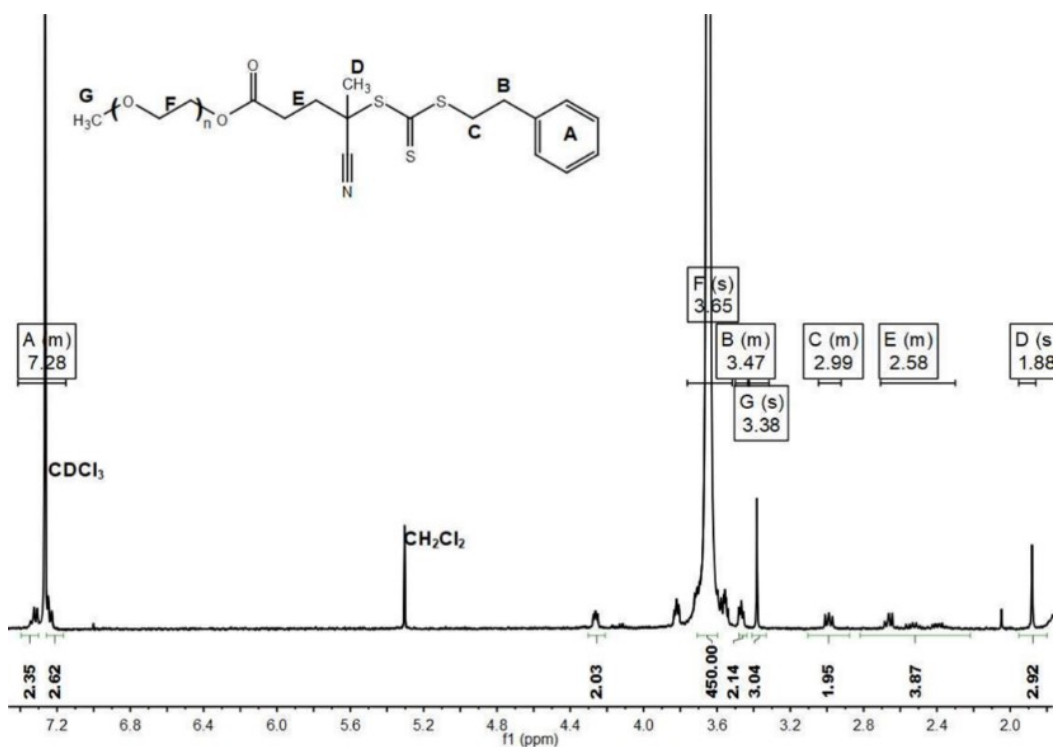
Supplementary Figure S5. ^1H NMR spectra (400 MHz, CDCl_3) and GPC traces in DMF (inset image) of PDMA-PF.



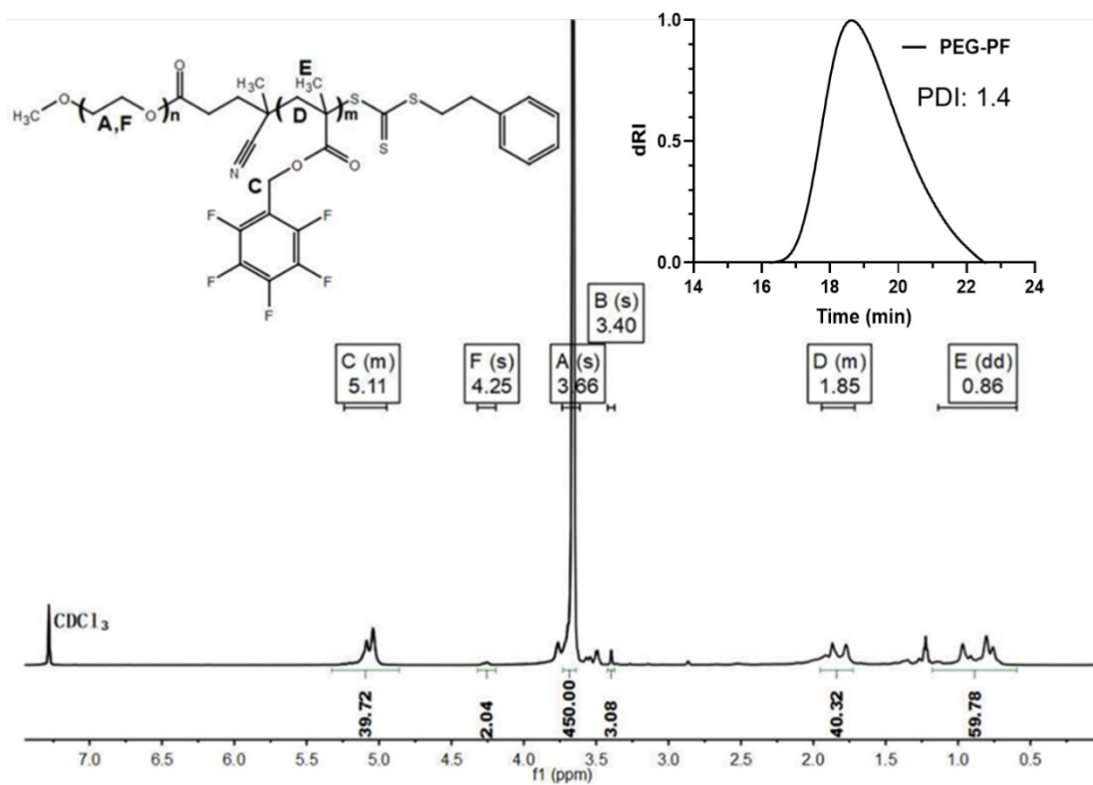
Supplementary Figure S6. ^1H NMR spectra of OPDMA-PF (400 MHz, DMSO- d_6).



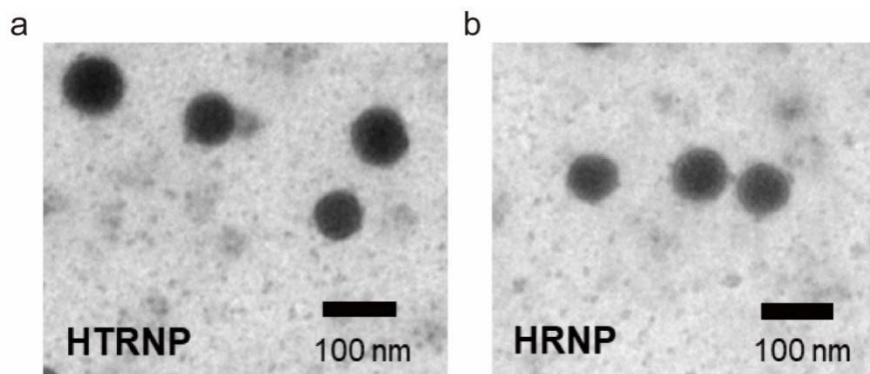
Supplementary Figure S7. Synthesis procedure of PEG-PF.



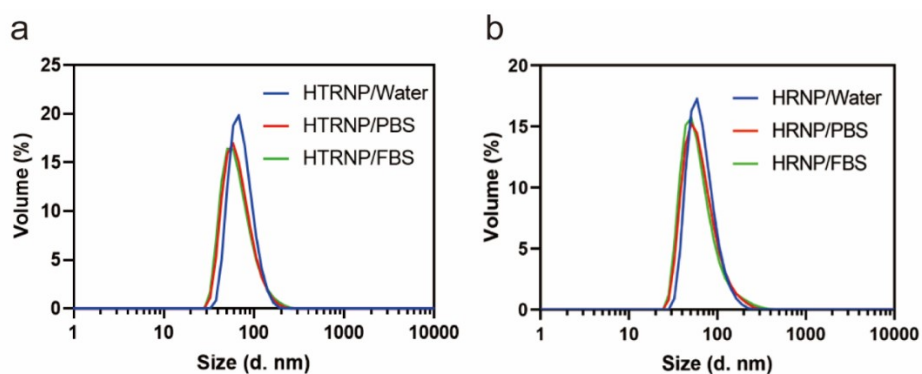
Supplementary Figure S8. ¹H NMR spectra of PEG_{5K}-PETTC (400 MHz, CDCl₃).



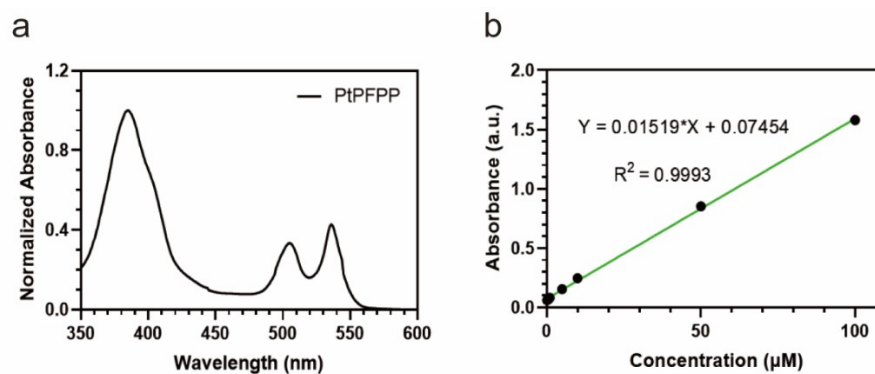
Supplementary Figure S9. ¹H NMR spectra (400 MHz, CDCl₃) and GPC traces in DMF (inset image) of PEG-PF.



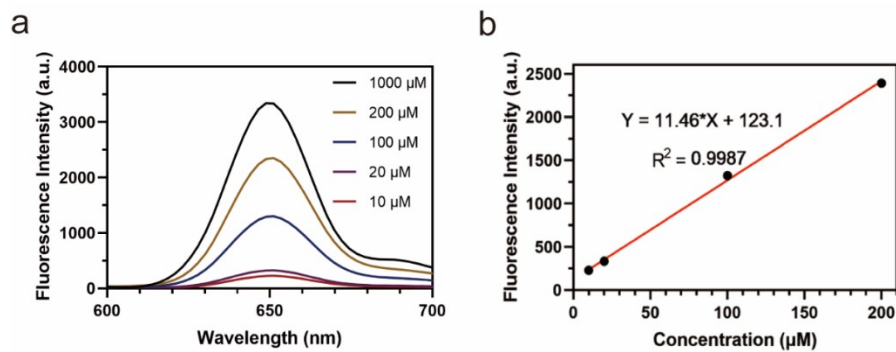
Supplementary Figure S10. The morphological characteristics of (a) HTRNP and (b) HRNP as observed through TEM, with a scale bar of 100 nm.



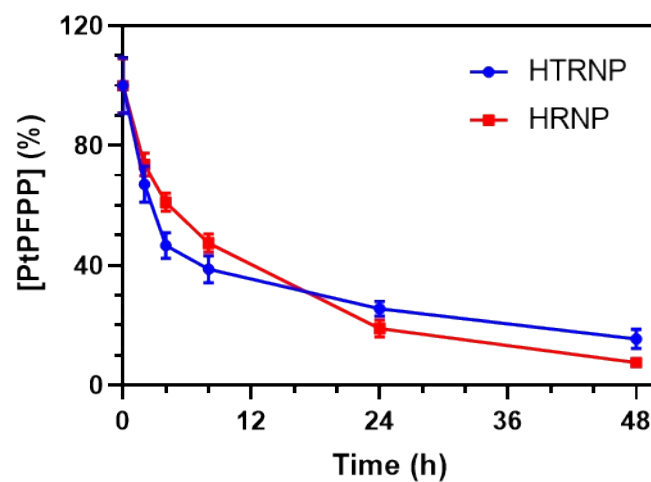
Supplementary Figure S11. The average particle size of HTRNP and HRNP. (a) The average particle size of HTRNP after 24 hours in water, PBS, and FBS as determined by DLS. (b) The average particle size of HRNP after 24 h in water, PBS, and FBS as determined by DLS.



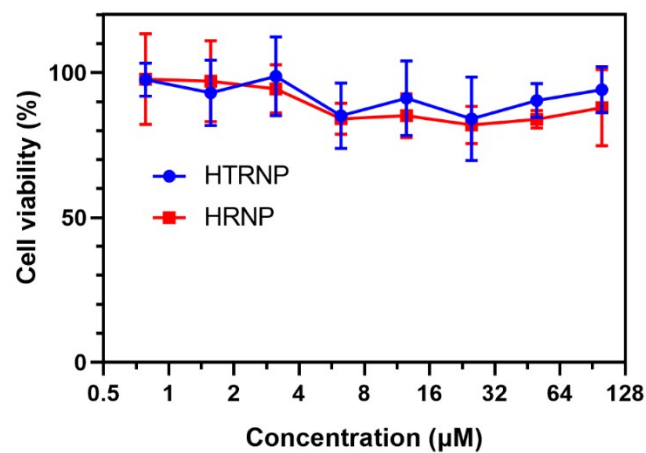
Supplementary Figure S12. Standard curve of absorbance with concentration of PtPFPP at 505 nm. (a) Standard absorption spectra of PtPFPP in DMSO. (b) Standard curve of characteristic absorbance value with concentration of PtPFPP at 505 nm in DMSO.



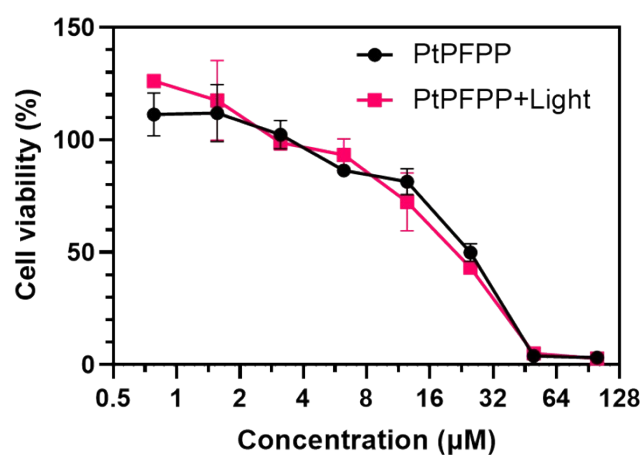
Supplementary Figure S13. Emission spectrum of HTRNP and phosphorescence intensity versus drug concentration relationship curve. (a) Emission spectra of HTRNP with different concentrations (10-1000 μM) at 540 nm excitation wavelength in aqueous solution. (b) Phosphorescence intensity versus concentration (10-200 μM) standard curve of HTRNP in aqueous solution at 540 nm excitation wavelength.



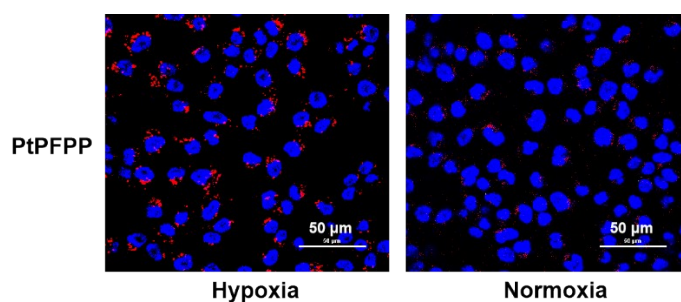
Supplementary Figure S14. Plasma clearance curves over 48 h of HTRNP and HRNP.



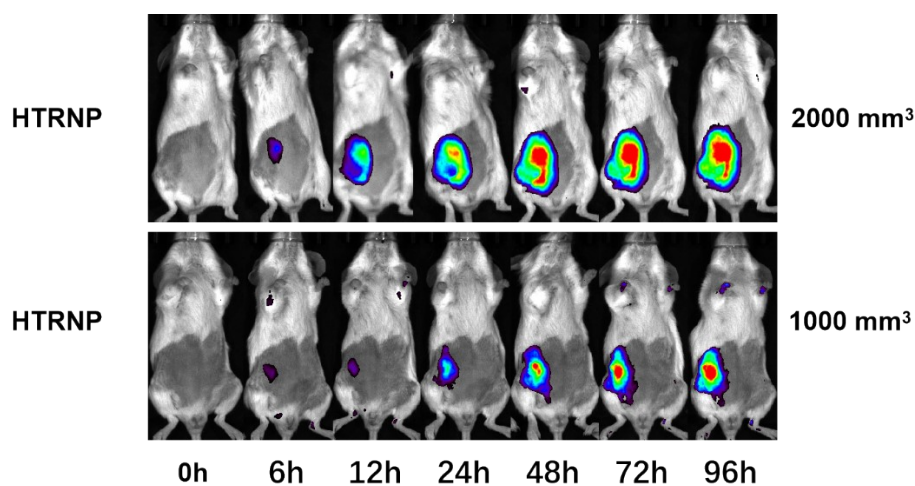
Supplementary Figure S15. The cytotoxic effect of the HTRNP and HRNP on 4T1 cell.



Supplementary Figure S16. The cytotoxic effect of the PtPFPP on 4T1 cell.



Supplementary Figure S17. Representative confocal images of 4T1 cells cultured with PtPFPP (10 μM) for 24 hours at 37 °C under hypoxia and normoxia. Nuclei stained with Hoechst 33342 were shown in blue, PtPFPP phosphorescence was shown in red. Excitation: 540 nm. Scale bars: 50 μm.



Supplementary Figure S18. Phosphorescence imaging of 4T1 orthotopic tumor-bearing mice with different tumor sizes (2000 mm³ or 1000 mm³ at 96 h after probe treatment) at different time points after tail vein injection of HTRNP (dosage: PtPFPP equivalent 1.5 mg/kg, 540 nm excitation, 670 nm emission).